

Molecular Dynamics in Binary Organic Glass Formers

Th. Blochowicz, C. Karle, A. Kudlik, P. Medick, I. Roggatz, M. Vogel, Ch. Tschirwitz, J. Wolber, J. Senker, and E. Rössler*

Physikalisches Institut, Universität Bayreuth, D-95440 Bayreuth, Germany

Received: September 17, 1998

We investigated binary low-molecular-weight glass formers as model systems for mixtures of small and large molecules. Tricresyl phosphate (TCP) in oligomeric styrenes (OS), benzene in OS and polystyrene (PS), and benzene in TCP were studied by applying dielectric spectroscopy as well as ^1H , ^2H , and ^{31}P NMR spectroscopy. Temperatures above and below the glass-transition temperature (T_G) are covered. The dielectric loss of the small component appears broader the higher the molecular ratio M/m is, and the lower the TCP concentration and the lower the temperature are chosen. Close to T_G , extremely broad distributions of correlation times $G(\log \tau)$ result, which are similar to those reported in the cases of polymer–plasticizer systems, although for our systems the motional heterogeneities are already established at similar M and m . By applying ^1H and ^2H (1D and 2D) NMR on benzene in OS and PS, we can demonstrate that the large molecules basically behave as in neat glass formers. However, the small molecules exhibit an isotropic reorientation also well below T_G , and the dynamics is rather characterized by a random jump process than by rotational diffusion, the latter being found in neat systems. Furthermore, we can prove that within $G(\log \tau)$, exchange processes take place, even below T_G , which essentially occur on the same time scale as reorientation.

Introduction

In the last few decades, the dynamics of simple organic glass formers has been thoroughly investigated by numerous experimental techniques. In particular, starting in 1984, the promising approach of mode coupling theory to describe the glass-transition phenomenon has prompted many new experiments. In contrast to neat systems, however, binary glass formers comprising two species of molecules have been studied to a lesser extent. Of course, many experimental data have been compiled for polymer–plasticizer systems^{1–14} or polymer blends.^{15–17} To our knowledge, a systematic comparison between binary and neat low-molecular-weight glass formers is still missing. Also, many dielectric studies are found that investigate a nonpolar low-molecular-weight glass former by dissolving a polar molecule, and it is usually believed that the polar molecules probe the dynamics of the glass former, although often a considerable amount of the polar substance is added.^{18–20} The present contribution focuses on the dynamics in binary low-molecular-weight glass formers by applying two techniques, namely, nuclear magnetic resonance (NMR) and dielectric spectroscopy.

Before turning to binary systems, one should briefly consider the essential characteristics of the glass transition in neat simple glass formers. In detail, this question is not easily answered, because, for a variety of relaxational features, universality and significance for the glass transition are still discussed controversially. Examples of this are the scaling and line shape of the main relaxation process (α process)^{21,22} or universality and significance of the Johari–Goldstein β relaxation.^{18,23} For the purpose of this contribution, however, it suffices to state on a very basic level that slow dynamics in simple glass formers (usually observed in the thermodynamically metastable state) is characterized by a main relaxational process (α process) exhibiting (i) a correlation time (τ_α) proportional to viscosity (η) and (ii) a spectral shape somehow broader than the Debye

relaxation with a width not changing significantly while cooling. The latter observation is often called the frequency–temperature superposition (FTS) principle.^{21,22} Note that, in particular statement i can be taken for granted only in the first approximation. Finally, concerning the reorientational motion of the molecules, multidimensional NMR experiments^{24,25} have recently proven that (iii) the motional mechanism is basically described by rotational diffusion with an elementary angle of finite size on the order of 10° . Conventionally, the relaxation spectrum of the α process is described by assuming a distribution of correlation times $[G(\log \tau)]$, and it is believed that dynamic heterogeneities underlie the α relaxation; that is, fast and slow molecules are subject to exchange processes. NMR^{26–28} and dielectric hole-burning methods²⁹ have demonstrated that these exchange processes occur on the same time scale as τ_α . Of course, one has to keep in mind that many relaxational features of simple glass formers are also shared by glassy crystals. In the case of ethanol, for example, it was recently demonstrated that the dielectric loss in the supercooled liquid and in the supercooled plastically crystalline phase is virtually indistinguishable.³⁰

The dynamics of binary glass formers is expected to depend on composition, size difference of the participating molecules, and temperature. Thus, a large amount of data has to be compiled in order to gain a consistent picture. Considering a situation of a mixture of small and large molecules, the possibility of a separation of time scales of small and large molecules has to be envisaged. Indeed, this is observed in polymer–plasticizer systems,^{1,4,6,8–14} and for some of these systems, even two glass transitions are reported in a restricted range of composition.^{3,5,9–11} Furthermore, the distribution of correlation times of the plasticizer is very broad, and the width was found to increase upon cooling.^{4–6,8–12,14} Usually, these features are explained by the presence of large concentration fluctuations.¹⁴ Also, the question may arise what kind of motion

persists in the glassy state. For example, the small molecules may undergo some kind of restricted motion within the frozen matrix of the large molecules. Again in the case of polymer–plasticizer systems, several authors have drawn this conclusion.^{6,7} We also want to note that colloidal systems comprising particles of significantly different radii³¹ and Lennard-Jones systems described within mode coupling theory²¹ show decoupled motion of the small component, and even the possibility of a second kind of glass transition of the small component in the glassy matrix of the large molecules is discussed by theory.^{32–34}

While it is difficult to extract the kind of reorientational process present from light-scattering and dielectric spectroscopy experiments, NMR is able to unravel the way the molecules reorientate.³⁵ Moreover, the high selectivity of NMR by introducing labeled components can be used in order to study both components in a given binary system. Here, we will focus on ¹H, ²H, and ³¹P NMR, in particular, two-dimensional (2D) NMR. In addition, the dielectric relaxation behavior is monitored. The mixtures studied are benzene in oligomeric styrene (OS) and in polystyrene (PS), tricresyl phosphate (TCP) in different oligomeric styrenes, and benzene in tricresyl phosphate. We note that the polymer–plasticizer system TCP/PS was already studied by dielectric,⁶ mechanical,⁵ and calorimetric^{9–11} experiments. Applying oligomeric styrenes with different molecular weights as molecularly large components provides a model system for binary glass formers of small and large molecules and, furthermore, enables us to study the crossover from low-molecular-weight mixed systems to polymer–plasticizer systems.

In the present work, we mainly focus on the relaxation behavior of the respectively smaller component of a binary mixture above and below the glass transition temperature, and we want to demonstrate that the dynamics is distinguished from the behavior of neat glass formers and that binary glass formers are well-suited model systems for studying dynamical heterogeneities. That is, in addition to monitoring the distribution of correlation times [$G(\log \tau)$], 2D NMR allows us to probe exchange processes within $G(\log \tau)$ as previously reported.³⁶ Most importantly, we will show that many effects found in polymer–plasticizer systems are already observed in low-molecular-weight mixtures.

Experimental Section

(i) **Samples.** An isomeric mixture of tricresyl phosphate ($m = 368$) was purchased from Aldrich and used for the dielectric investigations, whereas *m*-TCP (Kodak) was chosen for the NMR experiments. The glass dynamics of both systems is very similar;³⁷ for example, the glass transition temperature of *m*-TCP is only 5 K lower than that of the isomeric TCP. Because of this small difference, we will apply the abbreviation “TCP” in both cases. The various oligomeric and polymeric styrenes were obtained from Polymer Standard Service, and deuterated benzene (benzene-*d*₆) was obtained from Aldrich. All substances were used without further purification. The compounds were added together and kept in vacuum at temperatures between 80 and 150 °C for at least 24 h to ensure complete mixing and then used for the dielectric experiments. The NMR samples were directly prepared in a NMR glass tube and finally sealed off under weak vacuum. In all cases, homogeneous mixtures were prepared; i.e., no indication of phase separation was observed for the samples studied. All samples were characterized by carrying out differential scanning calorimetric (DSC) experiments on a Netzsch DSC 200. Figure 1 presents the heating

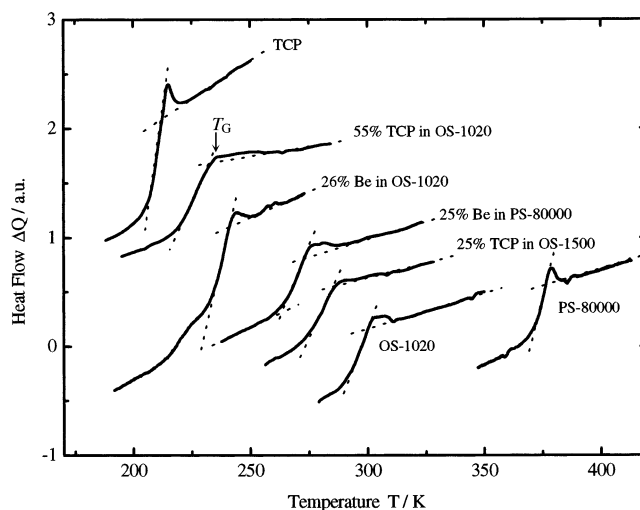


Figure 1. DSC traces for some of the systems studied. Dashed lines indicate the way the glass transition temperature (T_G) was determined; curves are arbitrarily shifted to each other.

TABLE 1: Systems Studied

systems	$c/\text{wt } \%$	T_G/K	M/m
OS-1020		299	1020
OS-2280		347	2280
PS-80000		376	80 000
benzene- <i>d</i> ₆ in OS-1020	26	240	1020/84
benzene- <i>d</i> ₆ in PS-80000	25	273	80 000/84
<i>m</i> -TCP		212	368
TCP		216	368
TCP in OS-269	54		269/368
TCP in OS-435	53		435/368
TCP in OS-1020	55	234	1020/368
TCP in OS-1500	25	287	1500/368
TCP in OS-1500	34	273	1500/368
TCP in OS-1500	51	257	1500/368
TCP in OS-1500	66	238	1500/368
TCP in OS-1500	94		1500/368
TCP in OS-2280	50	262	2280/368
TCP in OS-2280	66		2280/368
TCP in PS-80000	53	268	8000/368
benzene- <i>d</i> ₆ in TCP	8.2	205	368/84

curves (10 K/min) for neat TCP, PS, and OS ($M = 1020$) and four binary glass formers. Whereas the neat glass formers exhibit a sharp step in the heat capacity, the binary systems are characterized by significantly broader DSC traces. At high TCP concentrations ($c_w > 80\%$), we find indications for two glass-transition temperatures. The DSC results are similar to those reported by Pizzoli et al.⁹ In order to make a comparison possible between different systems, we define T_G as the end temperature of the heat capacity step while heating. This is also indicated in Figure 1.

Table 1 compiles c_w (by weight percent), T_G , and the molecular weight (number-average) of the oligomeric or polymeric styrene. In the following, M and m signify the molecular weight of the respective larger and smaller component in the binary mixture.

(ii) **Dielectric Spectroscopy.** The complex dielectric permittivity $\epsilon(\nu) = \epsilon'(\nu) - i\epsilon''(\nu)$ was measured for the system TCP in oligomeric and polymeric styrene at different concentrations and temperatures. As the dipole moment of styrene is negligible compared to that of TCP, the dielectric permittivity directly shows the reorientational dynamics of TCP, i.e., in most cases, the smaller component of the binary mixture. Measurements were carried out in the frequency range 10^{-2} – 10^9 Hz. For frequencies below 3×10^6 Hz, we used an SI 1260 impedance

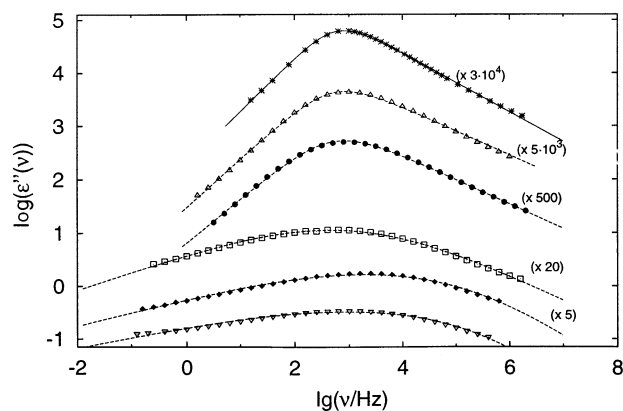


Figure 2. Dielectric loss curves of tricresyl phosphate (TCP) in various oligomeric styrenes (OS); (*) neat TCP, 233 K; (Δ) 54% TCP in OS-269, 224 K; (\bullet) 53% TCP in OS-435, 240 K; (\square) 51% TCP in OS-1500, 255 K; (\blacklozenge) 50% TCP in OS-2280, 262 K; (∇) 53% TCP in PS-80000, 263 K; numbers indicate vertical shift applied; solid line, interpolation by a Cole–Davidson susceptibility; dashed lines, fit with a Havriliak–Negami function.

analyzer from Schlumberger together with a broad-band dielectric converter from Novocontrol. At higher frequencies (3×10^5 – 3×10^9 Hz), a HP 8753C network analyzer from Hewlett-Packard was applied as a coaxial reflectometer.

(iii) NMR. The ^2H NMR and ^{31}P NMR experiments at $T > 200$ K were carried out on a Bruker DSX 400 spectrometer with a magnetic field of 9.4 T corresponding to a Larmor frequency of 61.4 MHz for deuterium and 161.9 MHz for phosphorus. A flow of cold nitrogen gas controlled by a Bruker VT 2000 heating device was applied to cool a commercial NMR probe (Bruker). The temperature stability was better than 1 K. The low-temperature 2D data of benzene- d_6 in OS were compiled on a Bruker CXP spectrometer upgraded with the Tecmag computer system operating at a ^2H Larmor frequency of 46.1 MHz, and a home-built NMR probe inserted in an Oxford cryostat CF 1200 was employed. Here, the temperature stability was better than 0.2 K. A solid-echo pulse sequence with a delay of 20 μs between the two pulses was applied to measure the ^2H NMR spectra (1D spectra). In the case of ^{31}P NMR, a Hahn-echo pulse sequence was chosen. Two-dimensional spectra were obtained by applying a five-pulse sequence with the phase cycle described in ref 38. Usually, the minimal 8-fold phase was applied. In some cases also, a 32-fold phase cycling was chosen in order to suppress contributions from single- and double-quantum coherences at short mixing times (t_m).³⁸ The delay between the first and the second pulses as well as between the fourth and the fifth pulses was set to 15 or 20 μs . The cosine and sine time signals were separately measured. After Fourier transformation, both data sets were added by applying a proper weighting factor.³⁵ The experimental spectra were symmetrized with respect to the diagonal, and a Gaussian broadening on the order of 1 kHz was introduced in order to improve the signal-to-noise ratio.

Results

(i) Dielectric Spectroscopy. We studied the dielectric loss of TCP in various oligomeric styrenes and in polystyrene. As said above, the dielectric response is dominated by that of the TCP molecules. Figure 2 displays the dielectric loss ($\epsilon''(\omega)$) of neat TCP and of TCP dissolved in styrenes with different molecular weights, where the displayed curves were chosen to yield a comparable average relaxation time. The concentration

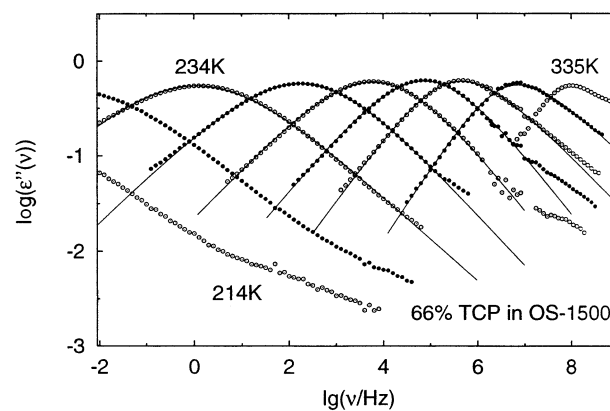


Figure 3. Evolution of dielectric loss of 66% tricresyl phosphate in oligomeric styrene (molecular weight 1500) with temperature; solid line, fit with a Havriliak–Negami function.

of the small component is approximately 50% (by weight) in each system. Whereas neat TCP can be described by a Cole–Davidson susceptibility, as is usually the case for neat glass formers, this is no longer possible for TCP in the mixed systems: by increasing the M of the oligomeric styrenes, the loss spectrum broadens considerably. An extremely broad loss is found for $M = 80\,000$. The broadening sets in already for an M that is comparable to that of TCP, and the curve for $M = 2280$ is virtually indistinguishable from the one for $M = 80\,000$. Thus, it becomes obvious that the broadening effect is not an polymer effect, but rather, it can be observed in mixed systems comprising molecules of different sizes, and some saturation is observed if the size difference (expressed, for convenience, by the molecular weight ratio M/m) exceeds a certain value.

We also investigated the dependence on the composition and found that the lower the TCP concentration is, the broader is the dielectric loss curve. At $c_w < 50\%$, indications for a bimodal loss curve are found with both relaxation peaks being very broad, similar to the results reported by Hains and Williams for TCP in PS.⁶ As in this case, it is difficult to clearly assign which part of the loss curve belongs to which relaxation process; we will describe the relaxation spectrum as a whole within the context of the present paper.

Figure 3 shows $\epsilon''(\omega)$ at different temperatures for 66% TCP in OS ($M = 1500$). While at high temperatures the relaxation spectrum is comparatively narrow, it is much broader at low temperatures. In order to describe the change of the dynamics upon cooling, we extracted $G(\log \tau)$ by first fitting the experimental curves by a Havriliak–Negami (HN) susceptibility function for $c_w > 50\%$ or a sum of two Cole–Cole (CC) functions for lower concentrations. The distribution of correlation times was then obtained by³⁹

$$G(\log \tau) = \frac{1}{2\pi\Delta\epsilon} \lim_{\omega \rightarrow 0} \{ \text{Im}[\epsilon(-\omega + i/\tau)] - \text{Im}[\epsilon(\omega + i/\tau)] \} \quad (1)$$

with $\Delta\epsilon$ being the relaxation strength.

The resulting logarithmic width (Δ) of $G(\log \tau)$ is displayed for various systems in Figure 4. Because T_G is significantly different for the different binary mixtures, the data are plotted on the reduced temperature scale (T_G/T). Clearly, extremely broad distributions as compared to those of neat glass formers are observed, and the FTS principle is strongly violated. The lower the concentration of TCP, the larger is the increase of the width while cooling. Furthermore, it becomes obvious that relaxation takes place also below T_G , and a change of the

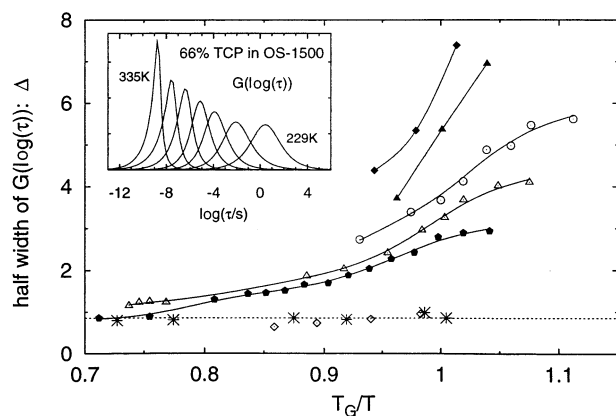


Figure 4. Half-width Δ of the distribution of correlation times, $G(\log \tau)$ as a function of reduced temperature T_G/T ; (*) neat TCP; (\diamond) 94% TCP in OS-1500; (\bullet) 66% in OS-1500; (\triangle) 51% TCP in OS-1500; (\blacktriangle) 34% TCP in OS-1500; (\blacklozenge) 25% in OS-1500; (\circ) 53% TCP in PS-80000; solid line, guide for the eye; dotted line, frequency temperature superposition principle as found in neat tricesyl phosphate. Inset: Evolution of $G(\log \tau)$ as a function of temperature in the case of 66% TCP in OS-1500.

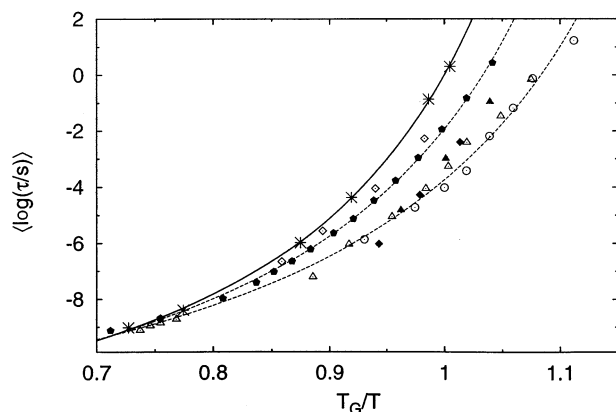


Figure 5. Mean logarithmic correlation time, $\langle \log \tau \rangle$, of tricesyl phosphate in various oligomeric styrenes, symbols as in Figure 4; solid line, neat TCP interpolated by a Vogel-Fulcher equation; dashed line, guide for the eye.

temperature dependence of $\Delta(1/T)$ close to T_G is observed: While at high temperatures ($T > T_G$) the overall glass transition of the binary system leads to a nonlinear temperature dependence of $\Delta(1/T)$, a smaller and rather linear $1/T$ dependence is revealed at $T < T_G$. A typical evolution of $G(\log \tau)$ with temperature is shown in the inset of Figure 4. Whereas at highest temperatures a narrow and somehow asymmetric $G(\log \tau)$ is observed, a behavior typical of neat glass formers, $G(\log \tau)$ becomes very broad and essentially symmetric at the lowest temperatures.

In Figure 5, the corresponding mean logarithmic time constant $\langle \log \tau \rangle$ is plotted as a function of the reciprocal temperature. Again, the reduced temperature scale is chosen in order to allow comparison. At the highest temperatures, the time constants are very similar for the different binary systems and close to the one of neat TCP. Approaching T_G , the TCP molecules in the mixed system relax significantly faster than in neat TCP at a given reduced temperature. The lower the temperature, the larger this difference becomes. For example, at $T = T_G$ for neat TCP, $\langle \log \tau/s \rangle \approx 0$, whereas $\langle \log \tau/s \rangle \approx -3$ for 51% TCP in oligomeric styrene ($M = 1500$). Once again, the relaxation process of the smaller component is also observed in the glass.

All together, the dynamics of the binary low-molecular-weight glass formers as it is shown by the dielectric experiments closely

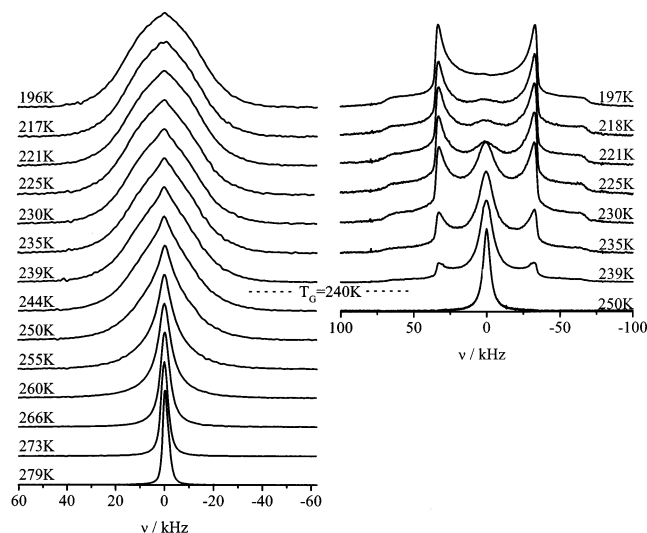


Figure 6. ^1H NMR spectra (left) and ^2H NMR spectra (right) for 26% benzene- d_6 in oligomeric styrene ($M = 910$); T_G is indicated.

resembles that observed in polymer-plasticizer systems. Furthermore, there are similarities in the dynamical behavior of the smaller component in the binary mixture to the reorientational dynamics of a supercooled liquid in the confined geometries of a nanoporous glass, especially with respect to the temperature dependence of width and correlation times.⁴⁰ Moreover, it becomes clear that a mixed system, even if it comprises two components, which do not significantly differ by size, may produce new relaxation effects. For example, in all mixed systems, no Debye behavior ($\epsilon''(\omega) \propto \omega$) is observed at the low-frequency side of the loss maximum.

Now we want to address the question of the nature of the distribution of correlation times. Is the dynamics homogeneous or heterogeneous, and what kind of motional mechanism characterizes the small component, in particular, below T_G ? These questions can all be answered by applying NMR techniques.

(ii) NMR. The mixed system 26% benzene- d_6 in polystyrene ($M = 910$) was studied by ^1H and, as previously reported,³⁶ by ^2H NMR. ^1H NMR probes the dynamics of polystyrene, whereas ^2H NMR reflects the motion of the benzene molecules. Figure 6 shows the corresponding spectra. The ^1H NMR spectra (left) are typical of a continuous slowing down of the segmental motion of the polystyrene molecules: A steadily broadening Lorentzian line is found at high temperatures, and slightly above T_G (240 K), the solid-state spectrum is established which, in the case of dipolarly coupled protons, is described by a Gaussian spectral shape in good approximation. The behavior is very similar to that observed for neat glass formers. The ^2H NMR spectra (right) exhibit a completely different behavior: Whereas at high temperatures the spectrum is again characterized by a Lorentzian line, near T_G traces of a solid-state spectrum, which, in the case of ^2H NMR is given by the Pake doublet reflecting the quadrupolar coupling of the spins (cf. also spectrum at $T = 197$ K), appear in addition to a broad Lorentzian line. Upon further cooling, the weight of the Lorentzian line declines, whereas the corresponding weight of the solid-state spectrum increases. Finally at $T = 197$ K, only a Pake doublet survives. The appearance of a Lorentzian line together with a solid-state spectrum below T_G shows that at least some benzene molecules undergo fast isotropic, liquid-like reorientation in the binary glass ($T < T_G$). Fast reorientation means that τ is significantly shorter than the reciprocal width of the solid-state spectrum ($1/\delta$); that is, $\tau < 10 \mu\text{s}$ in the case of ^2H NMR. In our previous

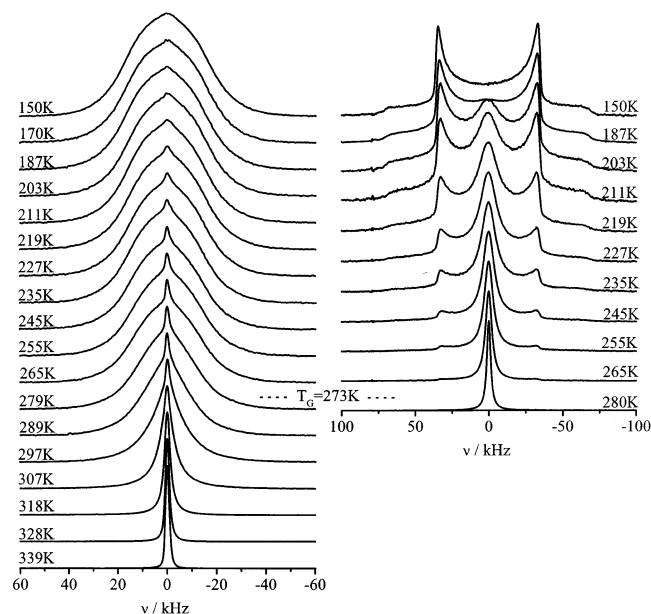


Figure 7. ^1H NMR spectra (left) and ^2H NMR spectra (right) for 25% benzene- d_6 in polystyrene ($M = 80\,000$); T_G is indicated.

work, we called such spectra, which can be described by a superposition of liquidlike (or, more generally, motionally averaged) and of a solidlike spectrum, two-phase spectra (cf. also ref 42). For convenience, we will apply this term also in this contribution.

Here, the question arises whether the fraction of benzene molecules contributing to the solid-state spectrum are actually rigid or whether they also perform isotropic reorientation, however on a longer time scale, for which the NMR line shape is not sensitive ($\tau \gg 10\,\mu\text{s}$). In the latter case, a very broad distribution of correlation times has to be assumed. By applying 2D NMR, we will show that this is indeed the case (cf. below). Of course, the presence of a broad distribution is also suggested by the results of the dielectric experiments discussed above. Then, the two-phase spectra observed are the mere effect of a very broad distribution of correlation times. Molecules with correlation times $\tau \ll 1/\delta$ yield a Lorentzian line and those with $\tau \gg 1/\delta$ contribute to a solid-state spectrum. Molecules with $\tau \approx 1/\delta$ can be neglected in the first approximation, because of a very broad distribution. Since the distribution $G(\log \tau)$ shifts with temperature, a continuously changing weighting factor, $W(T)$, representing the contribution of the Lorentzian line, in the range $0 < W(T) < 1.0$ is observed.^{41,42}

For comparison, we show in Figure 7 the corresponding ^1H and ^2H spectra for 25% benzene- d_6 in polystyrene ($M = 80\,000$). Very similar spectra are observed as in Figure 6. In the case of the polymer matrix, the temperature range where the motional heterogeneities of benzene show up in the NMR spectra is larger than for benzene in the low-molecular-weight styrene. As already demonstrated by our dielectric experiments, we find that the motional heterogeneities typical of polymer-plasticizer systems are rediscovered also in low-molecular-systems. In the case of polymer-plasticizer systems, two-phase spectra were already reported by several authors.^{1,8,12,13}

We mention that the actual width observed for the ^2H NMR spectra of benzene- d_6 is still reduced by a factor of 2 with respect to δ , because at all temperatures investigated here benzene performs fast rotational jumps around its 6-fold axis. Consequently, δ has to be substituted by the motionally averaged value $\bar{\delta}$ (cf. also eq 2). Thus, observing a liquidlike spectrum in the binary glass means that in addition to the fast reorientation

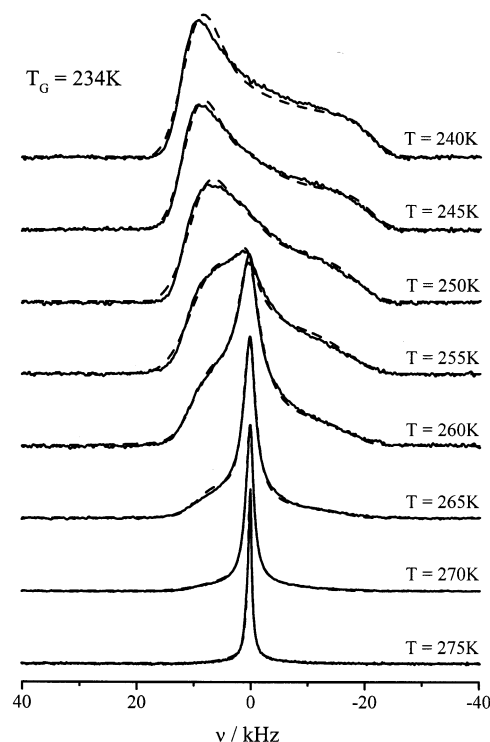


Figure 8. ^{31}P NMR spectra of 55% tricresyl phosphate in oligomeric styrene ($M = 1020\,\text{g/mol}$); T_G is indicated; dashed lines, interpolation by assuming two-phase spectra (cf. text).

around the symmetry axis, the axis itself reorients isotropically. Finally, we note that the small narrow line on top of the broad spectrum observed in the ^1H spectra in Figure 6 and Figure 7 is ascribed to the residual protons of the fast isotropically reorientating benzene- d_6 molecules.

In our dielectric relaxation study, we monitored TCP in oligomeric styrenes. As the TCP molecule contains a single phosphorus atom in its center, the molecule is well suited to study molecular reorientation by applying ^{31}P NMR. Figure 8 presents the corresponding spectra for 55% TCP in oligomeric styrene with $M = 1020$. Again, the spectra can be described by two-phase spectra as is also demonstrated in Figure 8 (dashed line). Dealing with a spin $I = 1/2$ for ^{31}P , the solid-state spectrum is determined by an axially symmetric chemical shift tensor and all spectra below T_G are asymmetric. Hetero- and homonuclear dipolar coupling introduce some additional broadening of the spectra. Thus, both TCP and benzene behave very similarly in the oligomeric matrix.

Obviously, the motional heterogeneities observed for the small component also show up in low-molecular-weight systems. We can further test this by looking at the ^2H and ^{31}P NMR spectra of a sample containing 8.2% benzene- d_6 in TCP displayed in Figure 9. In this case, TCP is the large component. Consequently, no two-phase ^{31}P spectra are found (left) but rather the NMR line continuously broadens while cooling, and finally, a chemical shift tensor spectrum shows up at the lowest temperatures, a behavior also found for neat TCP.⁴⁴ On the other hand, the ^2H spectra of benzene- d_6 exhibit features of two-phase spectra. However, in this case, the temperature interval, where these spectra are observed, is very small (and may easily be overlooked). We conclude that the distribution of correlation times becomes narrow when the size difference of the components is small.

Next we turn to 2D NMR experiments on benzene- d_6 in different styrenes. As mentioned, these experiments are sensitive for slow molecular dynamics and allow us to prove that the

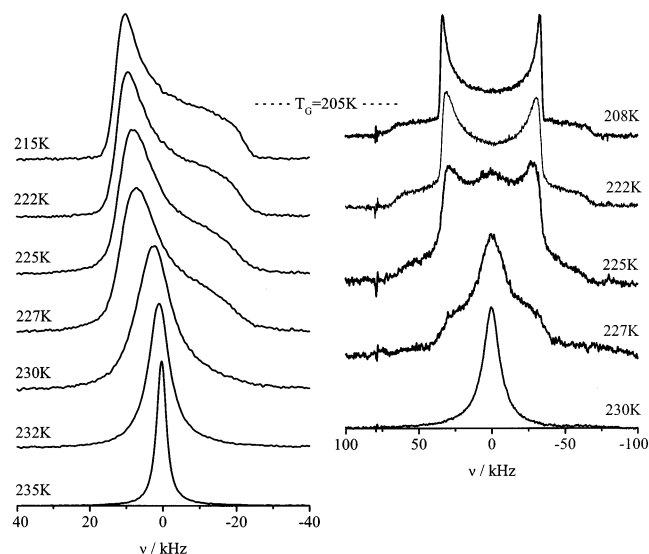


Figure 9. ^{31}P NMR (left) and ^2H NMR spectra (right) of 8.2% benzene- d_6 in tricresyl phosphate.

fraction of molecules contributing to the solid-state part of the two-phase 1D spectra (cf. Figures 6 and 7) still reorientate, but on a longer time scale ($\tau \gg 1/\delta$). In 2D NMR, reorientations with correlation times up to the spin–lattice relaxation time (T_1) are detectable. In the case of benzene, T_1 is determined by the fast reorientation around the 6-fold axis; i.e., a comparatively short T_1 on the order of some 100 ms is measured. Furthermore, as we will demonstrate, analyzing the 2D spectra also allows us to clarify the motional mechanism involved in the reorientation of the benzene molecules below T_G .

For the purpose of this study, it is sufficient to mention that a 2D spectrum probes the joint probability density [$P_{2|0}(\omega_1, \omega_2; t_m)$] to find NMR frequencies ω_1 at $t = 0$ and ω_2 at $t = t_m$ later, where t_m is the so-called mixing time chosen in the particular 2D experiment.³⁵ The NMR frequency is measured in the rotating frame and depends, in the case of ^2H NMR, on the orientation of the principal axes system of the electric field gradient tensor (specifying the quadrupolar interaction) with respect to the external magnetic field. As mentioned, this tensor is partially averaged by the fast reorientation of benzene around the 6-fold axis, resulting in an axially symmetric tensor with its principal axis pointing along the 6-fold axis of benzene. Then, the NMR frequency probes the orientation of the molecules via the relationship

$$\omega(\vartheta) = \pm(\bar{\delta}/2) [3 \cos^2(\vartheta) - 1] \quad (2)$$

where $\bar{\delta}$ is the motionally averaged width parameter of the quadrupolar interaction and ϑ the angle between magnetic field and 6-fold symmetry axis. Consequently, the 2D spectrum reflects the reorientation of the molecules on the time scale of the mixing time. $P_{2|0}(\omega_1, \omega_2; t_m)$ can be written as the product of the a priori probability density [$P_{1|0}(\omega_1)$] and the conditional probability density [$P_{1|1}(\omega_2; t_m|\omega_1)$]. The latter has to be calculated for the special type of motion considered, whereas in glasses, $P_{1|0}(\omega_1)$ is given by the normalized 1D powder spectrum, i.e., the Pake doublet spectrum.³⁵

Some special cases of motional processes are of interest here, and the calculations of the corresponding 2D spectra are well-known from the literature.^{35,36} For convenience, we display the calculated spectra in Figure 10. Assuming that no reorientation takes place ($\tau \gg t_m$), the 2D spectrum is given by a diagonal spectrum $S^{\text{dia}}(\omega_1, \omega_2)$, (cf. Figure 10a). For slow isotropic

reorientation ($1/\bar{\delta} \ll \tau \ll t_m$), a spectrum $S^{\text{reo}}(\omega_1, \omega_2)$ with off-diagonal intensity spread all over the ω_1/ω_2 plane (cf. Figure 10b) is found. In other words, the orientations of the molecules have equally redistributed over the surface of a sphere during t_m . Fast isotropic reorientation of the molecules averages out the orientational dependence of the quadrupolar interaction ($\tau \ll 1/\bar{\delta}$), and a Lorentzian line $S^{\text{Lor}}(\omega_1, \omega_2)$ is observed in the 2D spectrum as depicted in Figure 10c. Finally, a 2D spectrum $S^{\text{ex}}(\omega_1, \omega_2)$ as shown in Figure 10d results if a broad distribution of correlation times (yielding a two-phase 1D spectrum) is present within which exchange between fast ($\tau \ll 1/\bar{\delta}$) and slowly ($\tau \gg 1/\bar{\delta}$) reorientating molecules takes place. All these kinds of subspectra S^i will be observed in binary glass formers as we will demonstrate in the next section.

Figure 11 presents 2D spectra of 26% benzene- d_6 in oligomeric styrene with $M = 910$ at different temperatures below $T_G = 240$ K. At $T = 125$ K, a diagonal spectrum is observed, indicating that the molecules do not reorientate on the time scale of $t_m = 100$ ms. However, already at $T = 177$ K, i.e., well below T_G , off-diagonal intensity shows up in addition to a diagonal spectrum, indicating molecular reorientation. This off-diagonal contribution increases at higher temperatures, cf. spectrum at $T = 199$ K. At the highest temperature ($T = 218$ K), the off-diagonal pattern changes qualitatively. In addition to the spectral features just described, intensity along the frequency axes is observed.

First, we want to discuss the spectra below 218 K. At these temperatures, the 1D spectra are solely given by a ^2H NMR spectrum typical of the rigid symmetry axes of benzene; no signs of a Lorentzian line are discovered (cf. Figure 6). As demonstrated by the calculated spectra in Figure 11 (right hand), the measured spectra can be well reproduced by assuming a superposition of two subspectra discussed above, namely, the diagonal spectrum $S^{\text{dia}}(\omega_1, \omega_2)$ (cf. Figure 10a) and the spectrum $S^{\text{reo}}(\omega_1, \omega_2)$ typical of complete isotropic reorientation of the molecular axes (cf. Figure 10b):

$$S(\omega_1, \omega_2; t_m) \propto p_{\text{dia};t_m} S^{\text{dia}}(\omega_1, \omega_2) + p_{\text{reo};t_m} S^{\text{reo}}(\omega_1, \omega_2) \\ \text{with } p_{\text{dia};t_m} + p_{\text{reo};t_m} = 1 \quad (3)$$

The only parameter is the ratio of the weighting factors $p_{\text{dia};t_m}$ and $p_{\text{reo};t_m}$ specifying the weighting of the normalized spectra S^{dia} and S^{reo} , respectively. These weighting factors still depend on t_m , which is a parameter for a given 2D spectrum. Measuring the 2D spectra of the binary glass former for different t_m values, $p_{\text{reo};t_m}$ increases continuously starting from $p_{\text{reo};t_m} \approx 0$ at $t_m \approx 0$ and is expected to reach 1.0 at this temperature for very long mixing times, which actually cannot be measured due to a too short spin–lattice relaxation time. Thus, independent of mixing time and of temperature, again some kind of “two-phase” spectra are observed, making the analysis of the 2D spectra a very simple task. Together with the broad relaxation spectrum obtained from the dielectric experiments, we take the continuous increase of $p_{\text{reo};t_m}$ with rising mixing time as a clear proof that the dynamics of the small molecules is described by a broad continuous distribution $G(\log \tau)$.

The good agreement of the experimental results and the spectra obtained within this simple model deserves some explanation. As demonstrated by Spiess and co-workers,³⁵ within the motional model of rotational diffusion, even a broad distribution of $G(\log \tau)$ does not lead to the possibility to describe 2D spectra by applying eq 3, but rather a continuous broadening of the diagonal contribution is observed as a function

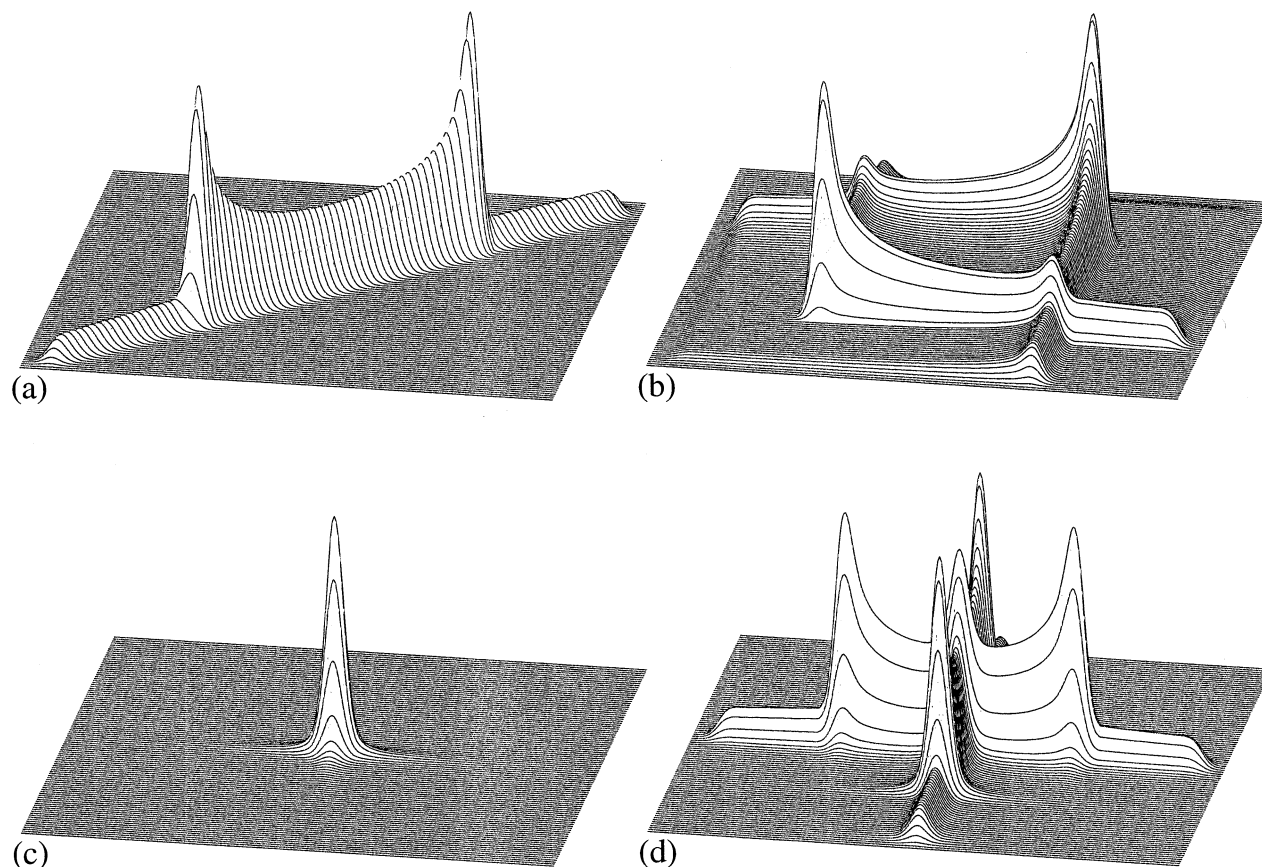


Figure 10. Typical 2D ^2H NMR spectra as obtained from calculations: (a) no motion; (b) slow isotropic reorientation ($1/\bar{\delta} \ll \tau \ll t_m$); (c) fast isotropic reorientation ($\tau \ll 1/\bar{\delta}$); (d) exchange between fast and slow reorientation.

of mixing time (cf. also ref 17). On the other hand, assuming isotropic random jumps, independent of the width of $G(\log \tau)$ and of the mixing time, a 2D spectrum can always be described by “two-phase” 2D spectra as given by eq 3.³⁵ This is due to the fact that for a random jump, the orientational correlation is lost with each jump process and, consequently, the intensity corresponding to a subensemble of molecules reorientating during t_m is distributed over the whole ω_1/ω_2 plane of the 2D spectrum. The weighting factor p_{dia,t_m} can be calculated³⁵ according to

$$p_{\text{dia},t_m} = \int_{-\infty}^{\infty} G(\log \tau) \exp(-t_m/\tau) d \log \tau \quad (4)$$

because for each τ at a certain t_m , the fraction of molecules which have not yet reorientated is given by $\exp(-t_m/\tau)$.

In order to compare the scenarios of a rotational diffusion and of a random jump more quantitatively, we calculated 2D spectra for both models and different mixing times using a $G(\log \tau)$ obtained from a separate measurement of the rotational correlation function at $T = 199$ K. Details concerning this measurement and the calculation will be presented in a forthcoming publication.⁴⁵ In Figure 12, we only show the results of the rotational diffusion (left) and random jump model (right), respectively. Clearly, the calculated 2D spectrum for $t_m = 100$ ms using the random jump model provides the better coincidence with the experimental 2D spectrum at 199 K for this mixing time. Therefore, we conclude that the motional mechanism of the small component in a binary glass former exhibits rather large angle reorientations whereas in a neat glass former reorientations, by small angular steps are predominant. This picture is also confirmed by preliminary results from studying the reorientational correlation functions in more

detail.⁴⁵ Of course, in the case of neat systems, rotational diffusion is found above T_G , i.e., in the supercooled liquid, while in the binary systems the random jump mechanism shows up below T_G . For the binary glass formers considered here, measuring 2D spectra above T_G does not yield information since the dynamics of the small component is too fast, leading to a 1D spectrum described solely by a Lorentzian line.

As is obvious from Figure 11 and already mentioned above, the 2D spectrum at 218 K shows higher intensity along the frequency axes than in the other off-diagonal area. This cannot be explained if only molecular reorientation is taken into account. Instead, as was demonstrated in our previous publication,³⁶ this spectral pattern is understood by also assuming exchange processes within the broad distribution of correlation times $G(\log \tau)$ present in binary glass formers. The new spectral feature is better resolved looking at the 2D spectra of 26% benzene in polystyrene ($M = 80\,000$) at $T = 225$ K as displayed in Figure 13 (left hand) and Figure 14 (left hand). A cut along the frequency axes of these spectra, i.e., for $\omega_1 = 0$ or $\omega_2 = 0$, yields, besides further intensity at the origin in each case, a Pake spectrum, and the additional intensity in the 2D spectra resembles that in Figure 10d. Fast-reorientating molecules at $t = 0$ ($\tau \ll 10$ μs) which have become sufficiently slow ($\tau \geq 1$ ms) during the mixing time contribute to a Lorentzian line in the ω_1 dimension and to a Pake spectrum in the ω_2 dimension. Thus, a Pake spectrum along $\omega_1 = 0$ is found. Vice versa, slow molecules at $t = 0$ which have become fast during t_m cause a Pake spectrum along the ω_2 axis. Thus, a crosslike off-diagonal pattern results. Therefore, also in this respect, benzene in oligomeric styrene and in polystyrene behaves similarly and an exchange of the correlation time is found below T_G . We emphasize that the exchange processes can only be studied in

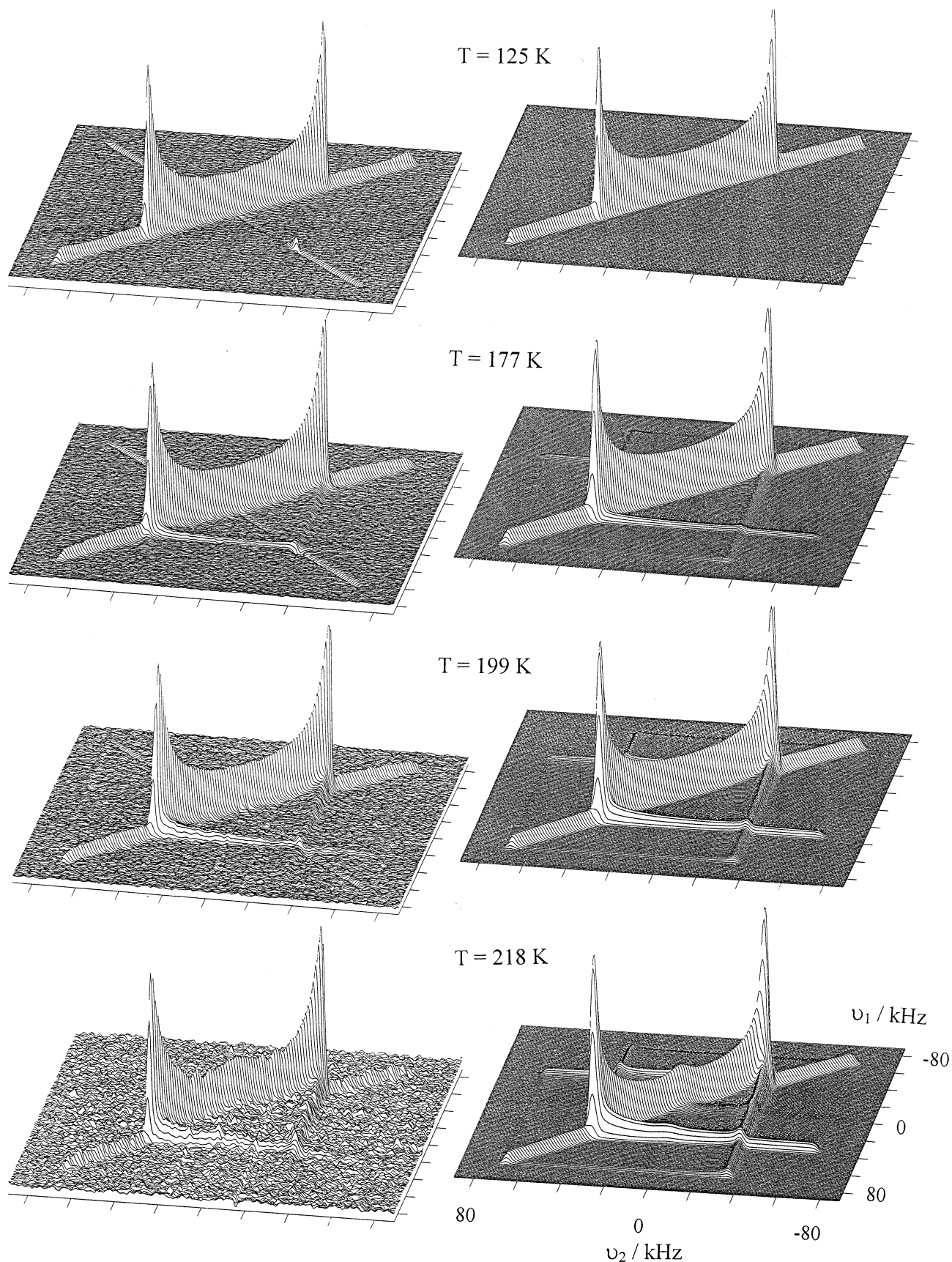


Figure 11. Experimental 2D ^1H NMR spectra (left) of 26% benzene- d_6 in oligomeric styrene ($M = 910$) for different temperatures and corresponding calculations (right); mixing time $t_m = 100$ ms; for increasing temperature, $p_{\text{diag}} = 1, 0.57, 0.33, 0.19$.

2D NMR provided that a Lorentzian line and a solid-state spectrum are simultaneously present in the 1D spectrum, as is the case in binary glass formers, however, not in neat systems.

In order to obtain the time scale of this exchange, the evolution of the 2D spectra for different mixing times in Figure 13 has to be analyzed quantitatively. We recently demonstrated

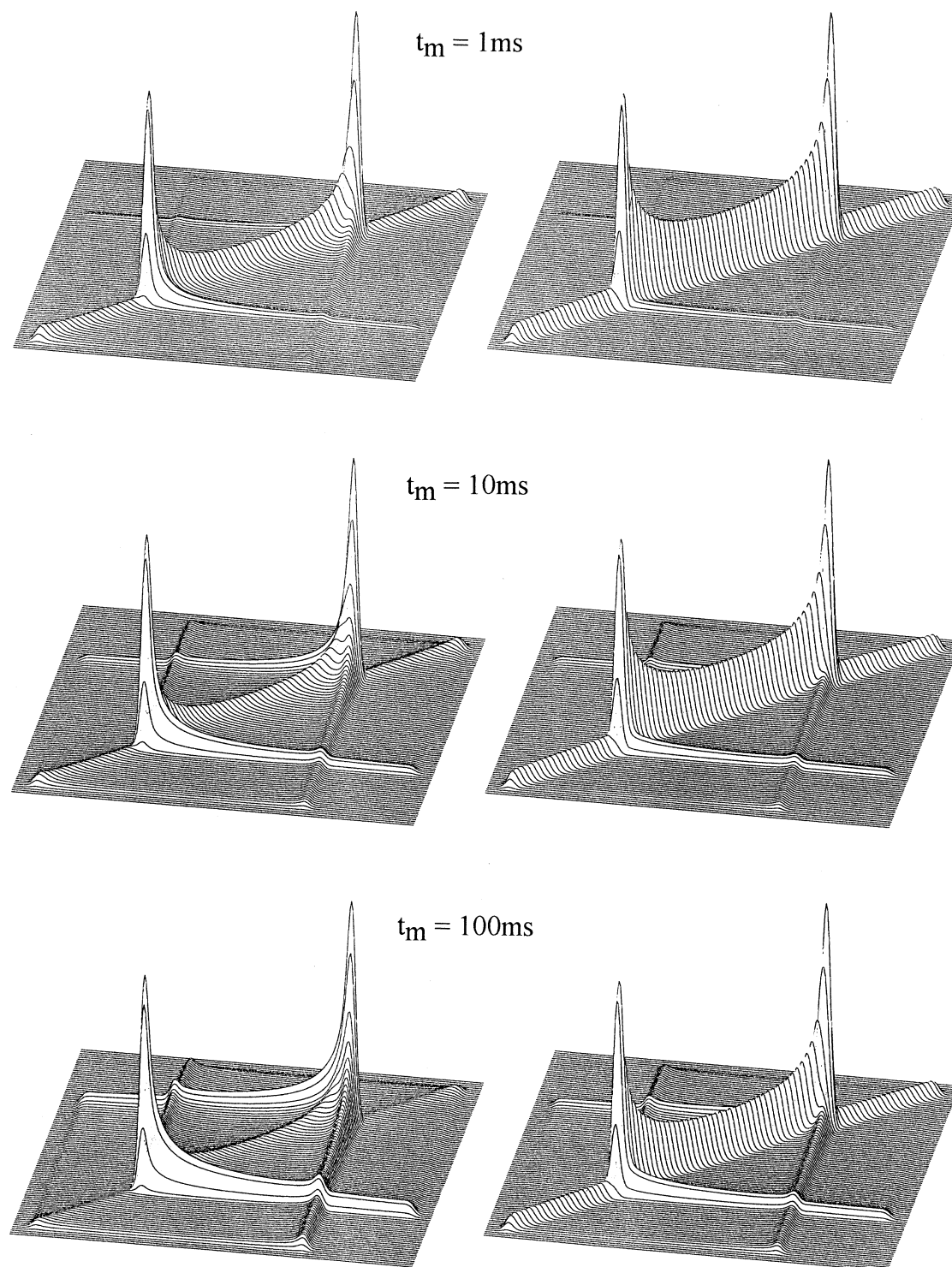


Figure 12. Theoretical 2D ^2H NMR spectra for the rotational diffusion model (left) and the random jump model (right), respectively, for different mixing times, t_m ($\langle\tau\rangle = 0.1$ s).

for benzene in oligomeric styrene that this can be simply done by describing the measured spectra as a weighted superposition of all of the above discussed subspectra³⁶

$$S(\omega_1, \omega_2; t_m) \propto p_{\text{dia};t_m} S^{\text{dia}}(\omega_1, \omega_2) + p_{\text{reo};t_m} S^{\text{reo}}(\omega_1, \omega_2) + p_{\text{Lor};t_m} S^{\text{Lor}}(\omega_1, \omega_2) + p_{\text{ex};t_m} S^{\text{ex}}(\omega_1, \omega_2)$$

$$\text{with } p_{\text{dia};t_m} + p_{\text{reo};t_m} + p_{\text{Lor};t_m} + p_{\text{ex};t_m} = 1 \quad (5)$$

The resulting calculated 2D spectra for the experimentally used

mixing times are also displayed in Figures 13 and 14 (right). By analyzing the mixing time dependence of the obtained weighting factors ($p_{\text{reo};t_m}$ and $p_{\text{ex};t_m}$), we are able to monitor the evolution of off-diagonal intensity originating from reorientational and from exchange processes separately. In Figure 15a, these two weighting factors together with $p_{\text{dia};t_m}$ for the system benzene- d_6 in polystyrene ($M = 80\,000$) are displayed. On the one hand, $p_{\text{dia};t_m}$ and, consequently, the relative intensity of the diagonal spectrum decline as t_m increases. On the other hand, $p_{\text{reo};t_m}$ and $p_{\text{ex};t_m}$ grow. At long mixing times, manifold exchange

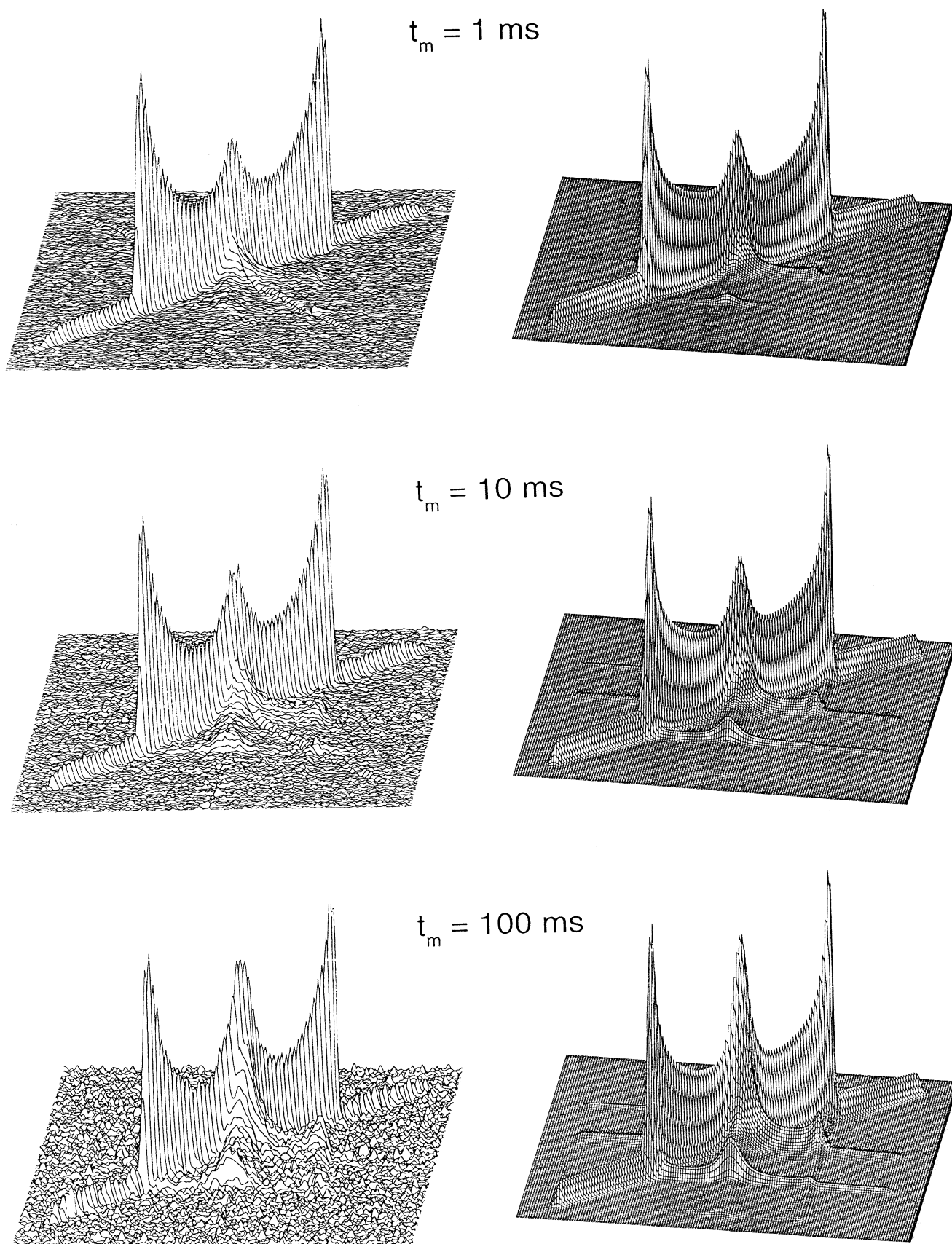


Figure 13. Experimental 2D ^2H NMR spectra (left) of 26% benzene- d_6 in polystyrene ($M = 80\,000$) for different mixing times, t_m , at $T = 225\text{ K}$ and calculations (right).

processes lead to a saturation behavior of $p_{\text{ex};t_m}$. However, for short mixing times, $t_m \leq 10\text{ ms}$, both $p_{\text{reo};t_m}$ and $p_{\text{ex};t_m}$ solely reflect reorientation and single exchange, respectively.³⁶ Looking

at $p_{\text{reo};t_m}$ and $p_{\text{ex};t_m}$ in Figure 15a in more detail, it becomes obvious that both increase in a similar manner. From that, we can conclude that reorientation and exchange processes occur

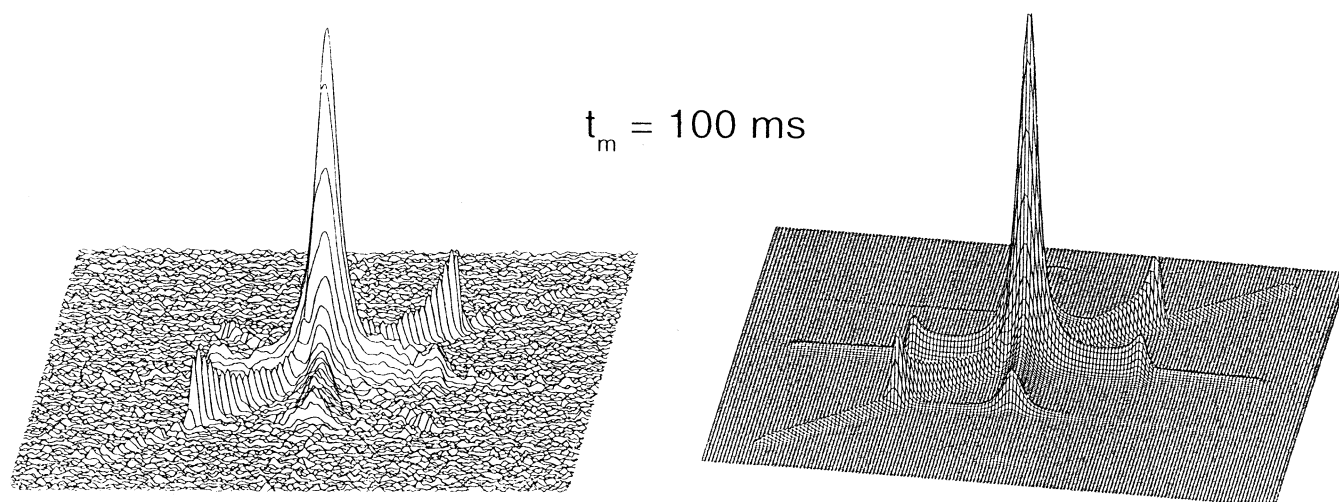


Figure 14. Experimental 2D ^2H NMR spectrum (left) of benzene- d_6 in polystyrene ($M = 80\,000$) at $T = 247\text{ K}$, mixing time $t_m = 100\text{ ms}$, and calculation (right).

on the same time scale. In other words, the benzene molecules in polystyrene do not remember their correlation times after a jump. The same result was found in our investigation on benzene in oligomeric styrene³⁶ and also, as mentioned, in neat systems.

Since the two-phase 1D spectra of benzene- d_6 in polystyrene cover a broad temperature range, we are able to look at the temperature dependence of the exchange, too. This was done by recording 2D spectra of benzene in polystyrene for different mixing times at a higher temperature, namely, at $T = 247\text{ K}$, and describing them also according to eq 5. The experimental (left) and the calculated (right) 2D spectra for $t_m = 100\text{ ms}$ are shown in Figure 14 as an example. The weighting factors $p_{\text{ex};t_m}$ obtained at $T = 225$ and 247 K together with those of benzene- d_6 in oligomeric styrene³⁶ are compiled in Figure 15b. However, in this figure, the factors $p_{\text{ex};t_m}$ are divided by $2W(1 - W)$, where W is the above-discussed weighting factor of the two-phase 1D spectrum. The term $2W(1 - W)$ represents the theoretically expected value of $p_{\text{ex};t_m}$ for $t_m \rightarrow \infty$,³⁶ and therefore, by scaling the values of the exchange intensity, the time scale of the exchange becomes more evident. In order to make the following discussion of our results more clear, we note that the exchange intensity observed in the 2D spectrum is caused by exchange processes which take place between correlation times $\tau \leq 1/\delta$ and $1/\delta \leq \tau \leq t_m$. Therefore, for short t_m , $p_{\text{ex};t_m}$ depends, on the one hand, on the fraction of molecules with correlation times $1/\delta \leq \tau \leq t_m$ (the population of molecules which can become fast, $\tau \leq 1/\delta$) and on the other hand, on the value of the exchange rate. In Figure 15b, it is obvious that the increase of $p_{\text{ex};t_m}$ for benzene- d_6 in oligomeric styrene is steeper than for benzene- d_6 in polystyrene. This is mainly due to the fact that for benzene in polystyrene, the observed distribution of correlation times is broader than for benzene in oligomeric styrene, as indicated by the larger temperature range of two-phase 1D spectra for benzene in polystyrene (cf. Figure 6 and Figure 7). Because of the narrower distribution in the case of benzene in oligomeric styrene, the fraction of molecules with correlation times $1/\delta \leq \tau \leq t_m$ grows faster if t_m is increased, leading to a larger slope of $p_{\text{ex};t_m}$. On the other hand, the exchange intensity of benzene- d_6 in polystyrene grows with a similar slope for both temperatures, but the curve at the higher temperature of 247 K is shifted to the left, i.e., to shorter times. A faster, increasing exchange intensity at higher temperatures indicates that the time scales of reorientation and exchange have a somehow different temperature dependence. This conclusion is obtained because the observed exchange takes place between the same correlation

times at both temperatures ($t_m = 1\text{--}100\text{ ms}$) and the fraction of molecules with these correlation times is similar because of the very broad distribution and the small change of the weighting factor. If the temperature dependence of exchange and reorientation are also the same, a similar time scale of the observed exchange at both temperatures will be expected, which is in contrast to the experimental result where the exchange at higher temperatures appears to be faster and, hence, indicates a trend that exchange and reorientation somehow decouple from each other. However, using this kind of 2D line-shape analysis, it is difficult to obtain absolute values of $p_{\text{ex};t_m}$ when comparing different systems or temperatures. Thus, relative errors of 20% are assumed and marked in Figure 15b. It is seen that in the worst case, the values at $T = 225$ and 245 K for mixing times $t_m \geq 10\text{ ms}$ can lie upon each other within the errors and one has to be cautious when interpreting our conclusion.

Looking once again at the 2D spectrum of benzene- d_6 in polystyrene at $T = 245\text{ K}$ displayed in Figure 14, it is obvious that only some diagonal intensity is left for a mixing time of 100 ms and the analysis according to eq 5 delivers $p_{\text{dia};t_m} = 0.15$. Therefore, 85% of the benzene molecules have reorientated isotropically after 100 ms . This is in contrast to the results discussed in the literature for the system TCP/PS.^{6,9} There it is assumed that a large fraction of TCP molecules is immobilized due to the presence of PS or undergo only hindered small-angle reorientations, i.e., a kind of secondary process. Instead, we assume that even the remaining 15% of the benzene molecules building up the diagonal intensity of the spectrum reorientate isotropically but on a time scale longer than the applied $t_m = 100\text{ ms}$. However, this cannot be proved because the spin-lattice relaxation time does not allow us to use much longer mixing times. Further, we want to mention that also for the systems TCP/OS investigated by ^{31}P 2D NMR no signs of remaining orientational correlation were observed,⁴⁵ clearly indicating that all molecules reorientate isotropically.

Discussion

Our combined dielectric and NMR study of binary low-molecular-weight glass formers reveals that these systems exhibit dynamics which is significantly different from that of neat glass formers. In particular, the molecularly smaller component is governed by pronounced motional heterogeneities, a behavior resembling that observed in polymer-plasticizer systems. These heterogeneities are more pronounced the lower

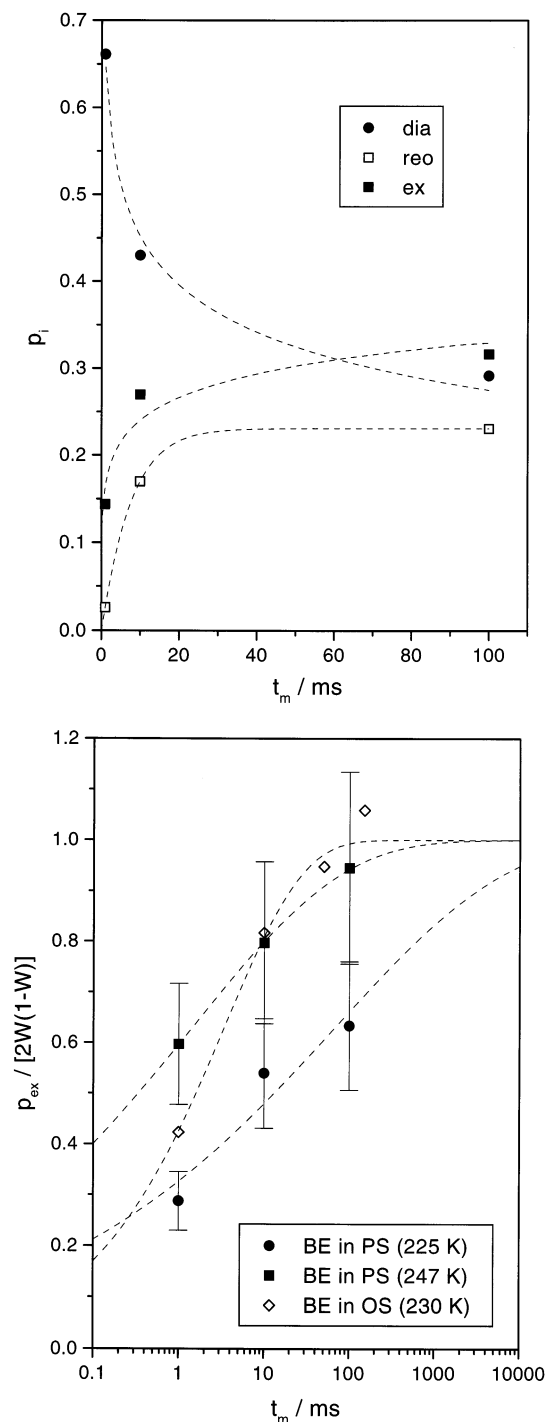


Figure 15. Weighting factors (p_i) as a function of mixing time obtained from analyzing the 2D spectra by eq 5: (a) the weighting factors as obtained for 25% benzene- d_6 in polystyrene; (b) normalized weighting factor (p_{ex}) characterizing exchange processes (cf. text) for benzene- d_6 in oligomeric styrene at $T = 230$ K and for benzene- d_6 in polystyrene at $T = 225$ and 247 K.

the concentration of small molecules ($25\% < c_{wm} < 100\%$) and the larger the ratio M/m becomes, and they directly show up in two-phase NMR spectra. Furthermore, the distribution of correlation times $G(\log \tau)$ becomes broader upon cooling, demonstrating a strong violation of the FTS principle. In this work, the ratio M/m was chosen as a measure of size difference. But as in simple glass formers, a scaling of mass with the glass-transition temperature is expected, the ratio of the glass-transition temperatures T_{GM}/T_{Gm} could be an equally suited parameter. Thus, we may conclude from our experiments that the nonuni-

form motion characteristic of polymer–plasticizer systems develops already in low-molecular-weight binary systems provided that the glass-transition temperatures of the respective neat compounds are sufficiently different.

Most importantly, we were able to show that motional heterogeneities of the small molecules are observed at temperatures far below T_G . In this case, molecular reorientation takes place in an essentially rigid matrix of large molecules, i.e., the small molecules perform a motional process decoupled from that of the polymer. Clearly, this means that the mean correlation time of the small molecules is no longer proportional to viscosity. Furthermore, below T_G , the width of $G(\log \tau)$ extracted from dielectric experiments appears to increase linearly with $1/T$, similar to the secondary relaxation process in neat glass formers (β process).²³ As proven by NMR, the motional mechanism in this temperature range is characterized by an isotropic random jump process, more precisely by large-angle motion, and exchange processes take place within the distribution $G(\log \tau)$.

In order to get some understanding of these findings, the following picture appears useful: Due to concentration fluctuations, regions exist with some small molecules being close to large molecules and some being close to other small molecules. Therefore, we could expect two different motional mechanisms to appear: single-particle motion and collective dynamics. For single-particle motion, which in particular should apply in the limit of low concentration, one can assume thermally activated reorientation, and the random jump mechanism may be taken as typical of small molecules moving within random potentials produced by large molecules. Accordingly, the width of the distribution of correlation times $G(\log \tau)$ should increase linearly with $1/T$, as might be anticipated from inspecting the data in Figure 4 ($T < T_G$). In this case, the exchange processes observed within $G(\log \tau)$ may be a mere effect from hopping processes in a random energy landscape. In addition to diffusion also small-angle fluctuations of the matrix can cause exchange, in the sense that the matrix reorganizes the potential probed by the small molecules. Indeed some indications for such slow fluctuations of the large molecules are found.⁴⁵

On the other hand, collective dynamics is supposed to dominate in the limiting case of high concentrations. For example, the investigations by Pizzoli et al.^{9,10} clearly demonstrate that two glass-transition temperatures can be identified at concentrations $0.35 < c_{wm} < 0.8$, one referring to polymer dynamics and the other to dynamics of the small molecules. This may indicate some reminiscence of the glass-transition dynamics even in the rigid polymer matrix. Thus, pronounced molecular dynamics in binary systems could be limited by T_{Gm} of the neat small components. Such a conclusion has been drawn by NMR investigations in the polymer–plasticizer system PS/toluene.⁸ Of course, also in the case of high concentrations, some small molecules are in contact with the large molecules and are somehow slowed down. Then, exchange of the correlation time can be interpreted as translational diffusion between locations more or less influenced by the large molecules and the small molecules behave quasi-liquid in the polymer matrix. However, diffusion cannot be probed by conventional NMR.

Of course, it remains unclear how both limiting mechanisms are combined in the intermediate concentration range and only at low concentrations can mere single particle dynamics be expected. Preliminary NMR results on benzene- d_6 in OS-1020 at $c_w = 3\%$ and 0.5% indicate that this crossover appears only at lower concentrations as the characteristics of the dynamics

still depend on concentration. Clearly, further experiments are needed to clarify the questions addressed here. In any case, it has become obvious that binary glass formers are systems worth being studied in their own right, and one has to be careful with drawing conclusions from studying the dynamics of small molecules dissolved in a glass former in order to probe the dynamics of the neat system.

References and Notes

- (1) Kosfeld, R. *Adv. Chem. Ser.* **1965**, 48, 49.
- (2) Ferry, D. J. *Viscoelastic Properties of Polymers*; Wiley: New York, 1980.
- (3) Braun, G.; Kovacs, A. J. *Physics of Non-crystalline Solids*; North Holland: Amsterdam, 1965; p 303.
- (4) Adachi, K.; Fujihara, I.; Ishida, Y. *J. Polym. Sci., Polym. Phys. Ed.* **1975**, 13, 2155.
- (5) Plazek, D. J.; Riande, E.; Markovitz, H.; Raghupathi, N. *J. Polym. Sci., Polym. Phys. Ed.* **1975**, 17, 2189.
- (6) Hains, P. J.; Williams, G. *Polymer* **1975**, 16, 725.
- (7) Desandro, M. A.; Walker, S.; Baarschers, W. H. *J. Chem. Phys.* **1980**, 73, 3460.
- (8) Rössler, E.; Sillescu, H.; Spiess, H. W. *Polymer* **1985**, 26, 203.
- (9) Pizzoli, M.; Scandola, M.; Ceccorulli, G. *Eur. Polym. J.* **1987**, 11, 843.
- (10) Ceccorulli, G.; Pizzoli, M.; Scandola, M. *Polymer* **1987**, 28, 2077.
- (11) Scandola, M.; Ceccorulli, G.; Pizzoli, M. *Polymer* **1987**, 28, 2081.
- (12) Jones, A. A.; Inglefield, P. T.; Liu, Y.; Roay, A. K.; Cauley, B. J. *J. Non-Cryst. Solids* **1991**, 131–133, 556.
- (13) Rössler, E.; Sillescu, H. In *Materials Science and Technology*; Cahn, R. W., Haasen, P., Kramer, E. J., Eds.; Verlag Chemie: Weinheim, 1991; Vol. 9.
- (14) Floudas, G.; Steffen, W.; Fischer, E. W.; Brown, W. *J. Chem. Phys.* **1993**, 99, 695.
- (15) Zetsche, A.; Fischer, E. W. *Acta Polym.* **1994**, 45, 168.
- (16) Katana, G.; Fischer, E. W.; Hack, Th.; Abetz, V.; Kremer, F. *Macromolecules* **1995**, 28, 2714.
- (17) Chung, G. -C.; Kornfield, J. A.; Smith, S. D. *Macromolecules* **1994**, 27, 5729.
- (18) Johari, G. P. *J. Chem. Phys.* **1970**, 53, 2372.
- (19) Shears, M. F.; Williams, G. *J. Chem. Soc., Faraday Trans 2* **1973**, 69, 1785.
- (20) Beevers, M. S.; Crossley, J.; Williams, G. *J. Chem. Soc., Faraday Trans. 2* **1977**, 73, 458.
- (21) Götze, W.; Sjögren, L. *Rep. Prog. Phys.* **1992**, 55, 241.
- (22) Ediger, M.; Angell, C. A.; Nagel, S. R. *J. Phys. Chem.* **1996**, 100, 13200.
- (23) Kudlik, A.; Tschirwitz, C.; Benkhof, S.; Blochowicz, T.; Rössler, E. *Europhys. Lett.* **1997**, 40, 649.
- (24) Böhmer, R.; Hinze, G. *J. Chem. Phys.* **1998**, 109, 241.
- (25) Hinze, G. *Phys. Rev. E* **1998**, 57, 2010.
- (26) Schmidt-Rohr, K.; Spiess, H. W. *Phys. Rev. Lett.* **1991**, 66, 3020.
- (27) Heuer, A.; Wilhelm, M.; Zimmermann, H.; Spiess, H. W. *Phys. Rev. Lett.* **1995**, 75, 2851.
- (28) Böhmer, R.; Diezemann, G.; Hinze, G.; Sillescu, H. *J. Chem. Phys.* **1998**, 108, 890.
- (29) Schiener, B.; Böhmer, R.; Loidl, A.; Chamberlin, R. V. *Science* **1996**, 274, 752.
- (30) Benkhof, S.; Kudlik, A.; Blochowicz, T.; Rössler, E. *J. Phys.: Condens. Matter*, in press.
- (31) Imhof, A.; Dhont, J. K. G. *Phys. Rev. E* **1995**, 52, 6344.
- (32) Franosch, T.; Götze, W. *J. Phys.: Condens. Matter* **1994**, 6, 4807.
- (33) Bosse, J.; Kaneko, Y. *Phys. Rev. Lett.* **1995**, 74, 4023.
- (34) Kaneko, Y.; Bosse, J. *J. Phys.: Condens. Matter* **1996**, 8, 9581.
- (35) Schmidt-Rohr, K.; Spiess, H. W., *Multidimensional Solid-State NMR and Polymers*; Academic: London, 1994.
- (36) Vogel, M.; Rössler, E. *J. Phys. Chem.* **1998**, 102, 2102.
- (37) Rössler, E.; Tauchert, J.; Eiermann, J. *J. Phys. Chem.* **1994**, 98, 8173.
- (38) Schaefer, D.; Leisen, J.; Spiess, H. W. *J. Magn. Reson. A* **1995**, 115, 60.
- (39) Böttcher, C. J. F.; Bordewijk, P. *Theory of Electric Polarization*; Elsevier: Amsterdam, 1978; Vol. II.
- (40) Arndt, M.; Stannarius, R.; Groothues, H.; Hempel, E.; Kremer, F. *Phys. Rev. Lett.* **1997**, 79, 2077.
- (41) Rössler, E.; Taupitz, M.; Vieth, H. M. *J. Chem. Phys.* **1990**, 92, 5847.
- (42) Rössler, E.; Taupitz, M. In *Disorder Effects on Relaxational Processes*; Richert, R., Blumen, A., Eds.; Springer: Berlin, 1994.
- (43) Resing, H. A. *J. Chem. Phys.* **1965**, 43, 669.
- (44) Rössler, E.; Eiermann, P. *J. Chem. Phys.* **1994**, 100, 5237.
- (45) Medick, P.; Vogel, M.; Wolber, J.; Rössler, E. To be published.